RESEARCH ARTICLE

Adenosine 2A Receptor Blockade as an Immunotherapy for Treatment-Refractory Renal Cell Cancer

Lawrence Fong[1], Andrew Hotson[2], John D. Powderly[3], Mario Sznol[4], Rebecca S. Heist[5], Toni K. Choueiri[6], Saby George[7], Brett G.M. Hughes[8], Matthew D. Hellmann[9], Dale R. Shepard[10], Brian I. Rini[10], Shivaani Kummar[11], Amy M. Weise[12], Matthew J. Riese[13], Ben Markman[14], Leisha A. Emens[15], Daruka Mahadevan[16], Jason J. Luke[17], Ginna Laport[2], Joshua D. Brody[18], Leonel Hernandez-Aya[19], Philip Bonomi[20], Jonathan W. Goldman[21], Lyudmyla Berim[22], Daniel J. Renouf[23], Rachel A. Goodwin[24], Brian Munneke[2], Po Y. Ho[2], Jessica Hsieh[2], Ian McCaffery[2], Long Kwei[2], Stephen B. Willingham[2], and Richard A. Miller[2]

ABSTRACT

Adenosine mediates immunosuppression within the tumor microenvironment through triggering adenosine 2A receptors (A2AR) on immune cells. To determine whether this pathway could be targeted as an immunotherapy, we performed a phase I clinical trial with a small-molecule A2AR antagonist. We find that this molecule can safely block adenosine signaling *in vivo*. In a cohort of 68 patients with renal cell cancer (RCC), we also observe clinical responses alone and in combination with an anti–PD-L1 antibody, including subjects who had progressed on PD-1/PD-L1 inhibitors. Durable clinical benefit is associated with increased recruitment of $CD8^+$ T cells into the tumor. Treatment can also broaden the circulating T-cell repertoire. Clinical responses are associated with an adenosine-regulated gene-expression signature in pretreatment tumor biopsies. A2AR signaling, therefore, represents a targetable immune checkpoint distinct from PD-1/PD-L1 that restricts antitumor immunity.

SIGNIFICANCE: This first-in-human study of an A2AR antagonist for cancer treatment establishes the safety and feasibility of targeting this pathway by demonstrating antitumor activity with single-agent and anti–PD-L1 combination therapy in patients with refractory RCC. Responding patients possess an adenosine-regulated gene-expression signature in pretreatment tumor biopsies.

See related commentary by Sitkovsky, p. 16.

[1]UCSF Helen Diller Family Comprehensive Cancer Center, San Francisco, California. [2]Corvus Pharmaceuticals, Burlingame, California. [3]Carolina BioOncology Institute, Huntersville, North Carolina. [4]Yale University Cancer Center, Yale University, New Haven, Connecticut. [5]Massachusetts General Hospital, Harvard University, Boston, Massachusetts. [6]Dana-Farber Cancer Institute, Boston, Massachusetts. [7]Roswell Park Cancer Institute, Buffalo, New York. [8]Royal Brisbane Hospital and University of Queensland, Herston, Brisbane, Queensland, Australia. [9]Memorial Sloan Kettering Cancer Center, New York, New York. [10]Cleveland Clinic Foundation, Cleveland, Ohio. [11]Stanford University School of Medicine, Stanford, California. [12]Karmanos Cancer Institute, Wayne State University, Detroit, Michigan. [13]Medical College of Wisconsin, Wauwatosa, Wisconsin. [14]Monash Health and Monash University, Melbourne, Clayton, Victoria, Australia. [15]UPMC Hillman Cancer Center, Pittsburgh, Pennsylvania. [16]University of Arizona Cancer Center, Tucson, Arizona. [17]University of Chicago Medical Center for Care and Discovery, Chicago, Illinois. [18]Icahn School of Medicine at Mount Sinai, New York, New York. [19]Washington University Siteman Cancer Center, St Louis, Missouri. [20]Rush University Medical Center, Chicago, Illinois. [21]Ronald Reagan UCLA Medical Center, Los Angeles, California. [22]University of Nebraska Medical Center, Omaha, Nebraska. [23]BC Cancer - Vancouver, Vancouver, British Columbia, Canada. [24]The Ottawa Hospital Cancer Centre, Ottawa, Ontario, Canada.

Note: Supplementary data for this article are available at Cancer Discovery Online (http://cancerdiscovery.aacrjournals.org/).

Corresponding Authors: Lawrence Fong, University of California, San Francisco, 513 Parnassus Avenue, Room HSE301A, San Francisco, CA 94143-0519. Phone: 415-514-3160; Fax: 415-476-0459; E-mail: Lawrence.Fong@ucsf.edu; and Richard A. Miller, Corvus Pharmaceuticals, 863 Mitten Road, Suite 102, Burlingame, CA 94010. Phone: 650-900-4520; E-mail: rmiller@corvuspharma.com

Cancer Discov 2020;10:40–53

doi: 10.1158/2159-8290.CD-19-0980

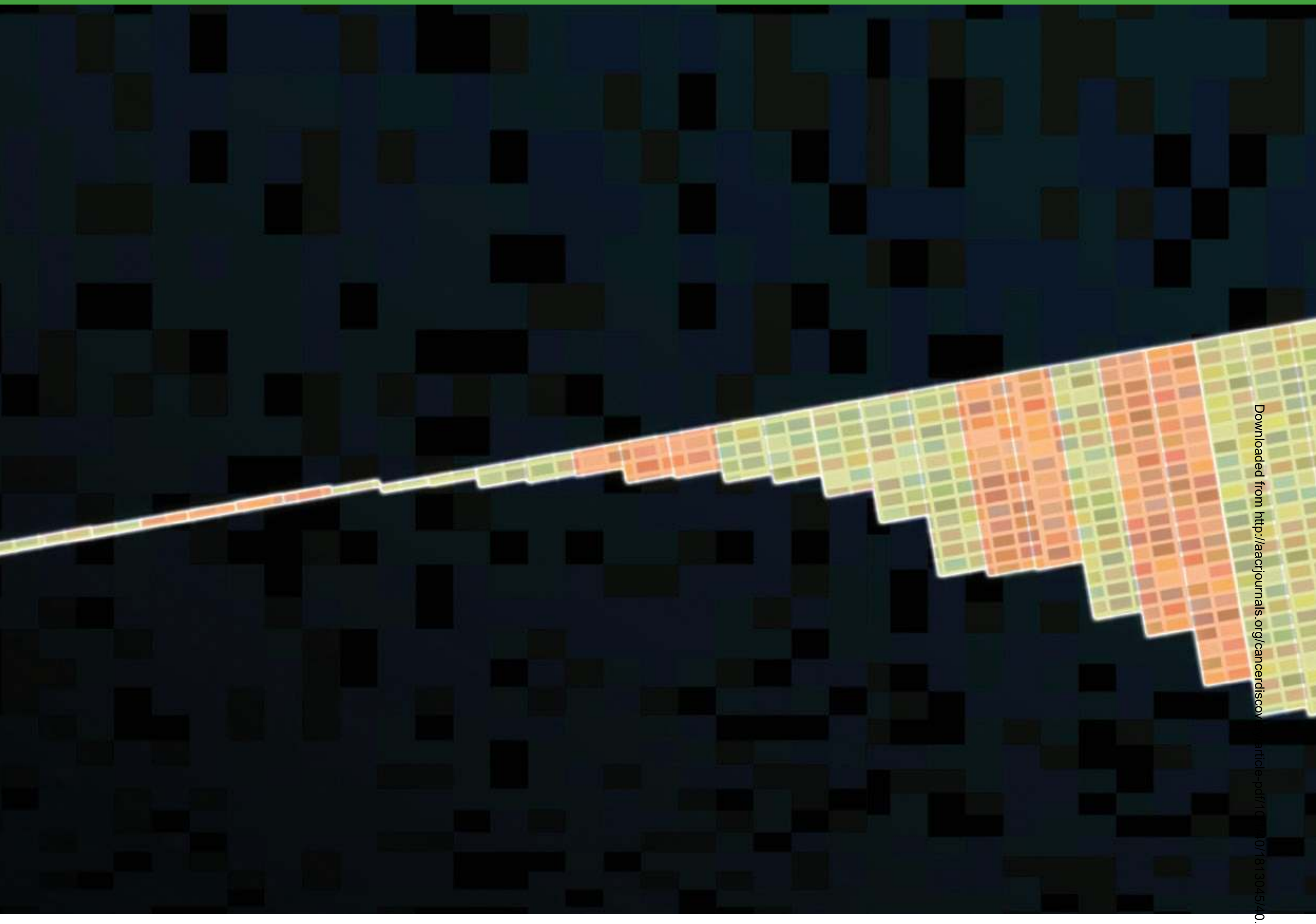

INTRODUCTION

Overcoming immunosuppressive barriers within the tumor microenvironment has become an important strategy in treating cancer in the era of immunotherapy (1). Accumulation of the nucleoside adenosine in the tumor microenvironment has been shown to inhibit the antitumor function of various immune cells, including cytotoxic T cells and natural killer cells, by binding to cell surface adenosine 2A receptor (A2AR; refs. 2–9). Adenosine further restricts antitumor immunity by augmenting the immunosuppressive activity of myeloid and regulatory T cells (10–13). Adenosine is generated in tumors through the coordinated activity of the ectonucleotidases CD39 (also known as ENTPD1) and CD73 (also known as 5′-NT and NT5E) that together convert extracellular adenosine triphosphate (ATP), an inflammation-inducing factor, to adenosine. In turn, adenosine inhibits the proinflammatory effects of ATP released by injured or dying cells, and its generation can be co-opted by tumors as a mechanism to suppress antitumor immunity (4, 14).

Renal cell carcinoma (RCC) may be particularly influenced by the effects of adenosine in the tumor microenvironment. The adenosine pathway genes *ADORA2A* (A2AR) and *NT5E* (CD73) are both highly expressed in RCC compared with other solid-tumor histologies (Supplementary Fig. S1). Intratumoral hypoxia may contribute to the production of extracellular adenosine in RCC tumors by upregulating CD39 and CD73 expression and stimulating the release of intracellular ATP (2, 15–18). Adenosine pathway genes may also be induced as a consequence of somatic mutations in the von Hippel–Lindau (VHL) gene, which are common in RCC, that increase levels of hypoxia inducible factor 1 (HIF1) and HIF2 activity to mimic conditions of intratumoral hypoxia (2, 16, 19).

The treatment landscape of RCC has evolved dramatically in recent years, with promising results and/or approvals for therapies targeting the PD-1/PD-L1 pathway alone or in combination with anti-CTLA4, VEGF inhibitors, and tyrosine kinase inhibitors (TKI; refs. 20–22). However, complete remissions remain uncommon and metastatic RCC is still by and large incurable, with responses short-lived in later lines of therapy.

Studies in animal models have shown that prior treatment with anti–PD-1 antibodies results in increased expression of A2AR and CD73, suggesting that the adenosine pathway may contribute to therapeutic resistance to immunotherapy (23, 24). There is a need for new combination therapies that prevent or overcome resistance to PD-1/PD-L1 blockade, and for biomarkers to identify and predict resistance mechanisms with the goal of selecting the most appropriate therapy.

Ciforadenant (previously known as CPI-444) is a small molecule that potently and selectively binds A2AR, and competitively inhibits the binding and signaling of adenosine (25). Ciforadenant has been shown to be active in multiple preclinical tumor models both as a monotherapy and in combination with anti–PD-1/PD-L1 (25, 26). We conducted a first-in-human phase I dose-escalation study with ciforadenant monotherapy and combination with atezolizumab in patients with advanced refractory cancers (Supplementary Fig. S2). The primary objectives were to (i) evaluate the safety and tolerability of multiple doses of ciforadenant administered on a daily schedule to subjects with selected incurable cancers as a single agent and in combination with atezolizumab, (ii) identify a recommended dose and schedule for further study of ciforadenant on the basis of safety, pharmacokinetic, and pharmacodynamic data, and (iii) evaluate the antitumor activity of ciforadenant as a single agent and in combination with atezolizumab. Secondary objectives included a characterization of ciforadenant pharmacokinetics, biomarkers associated with the efficacy or safety of ciforadenant, and progressive disease effects of ciforadenant on lymphocyte subsets, cytokine production, immune function, tumor IHC or gene-expression patterns. On the basis of the observation of early evidence of antitumor activity in patients with RCC, we expanded the study (phase Ib) to gain more experience with monotherapy and combination therapy in this disease. Here we report the safety and efficacy of adenosine blockade in patients with advanced refractory RCC. We have also identified a gene-expression signature that associates with treatment-related disease control, which may be useful as a predictive biomarker.

RESULTS

Patient Characteristics

A total of 68 patients with RCC were enrolled over a 24-month period ending in April 2018. Thirty-three patients received ciforadenant monotherapy and 35 patients received the combination of ciforadenant and atezolizumab. Median on-treatment time was 5 (1–21.7) months. Baseline demographics and disease characteristics are shown in Table 1. All patients had documented disease progression at the time of study entry and had failed multiple previous therapies (median = 3) including TKIs and anti–PD-1 antibodies (Table 1). More than 72% of patients were resistant or refractory to previous anti–PD-1/PD-L1 antibody treatment; median time since last dose of anti–PD-1/PD-L1 was 3.1 months (range, 1.2–70.4 months) and 1.7 months (range 0.9–23.6 months) for monotherapy and combination therapy cohorts, respectively (Table 1). Nine percent of evaluable patients had ≥ 5% PD-L1 expression on tumor or immune cells in pretreatment tumor biopsy specimens (Table 1).

Table 1. Baseline characteristics of all enrolled patients

Characteristics	Ciforadenant (*n* = 33)	Ciforadenant + atezolizumab (*n* = 35)
Age, years [median (range)]	60 (47–76)	65 (44–77)
Gender, male *n* (%)	25 (75.8)	28 (80)
Sites of disease, *n* (%)		
Lung	22 (66.7%)	27 (77.1%)
Lymph node	19 (57.6%)	21 (60%)
Bone	16 (48.5%)	15 (42.9%)
Liver	10 (30.3)	9 (25.7%)
Number of prior therapies		
Median, range	3 (1, 5)	3 (1, 5)
Prior IO, number of subjects, *n* (%)	24 (72.7)	25 (71.4)
Months since prior IO		
Median, range	3.1 (1.2, 70.4)	1.7 (0.9, 23.6)
PD-L1 IHC status		
≥5% PD-L1$^+$ on TC or IC, *n* (%)	2/27 (7.4%)	3/31 (9.7%)
Prior anticancer therapy, *n* (%)		
TKI	27 (81.8)	30 (85.7)
mTOR	9 (27.3)	11 (31.4)
Anti–PD-1	23 (69.7)	25 (71.4)
Anti-VEGF, bevacizumab	6 (18.2)	4 (11.4)
IL2	7 (21.2)	9 (25.7)

Abbreviations: IO, immunotherapy; TC, tumor cells; IC, immune cells.

Table 2. Treatment-related adverse events

	Ciforadenant ($n = 33$)		Ciforadenant + atezolizumab ($n = 35$)	
Event, number of patients, (%)	Any grade	Grade 3/4	Any grade	Grade 3/4
Fatigue	13 (39.4)	0 (0.0)	16 (45.7)	0 (0.0)
Pruritus	7 (21.2)	0 (0.0)	9 (25.7)	0 (0.0)
Decreased appetite	4 (12.1)	1 (3.0)	6 (17.1)	0 (0.0)
Dizziness	4 (12.1)	0 (0.0)	1 (2.9)	0 (0.0)
Nausea	3 (9.1)	0 (0.0)	7 (20.0)	1 (2.9)
Pyrexia	3 (9.1)	0 (0.0)	1 (2.9)	0 (0.0)
Anemia	2 (6.1)	1 (3.0)	4 (11.4)	0 (0.0)
Arthralgia	2 (6.1)	1 (3.0)	5 (14.3)	1 (2.9)
Chills	2 (6.1)	0 (0.0)	1 (2.9)	0 (0.0)
Cough	2 (6.1)	0 (0.0)	3 (8.6)	0 (0.0)
Diarrhea	2 (6.1)	0 (0.0)	5 (14.3)	0 (0.0)
Epistaxis	2 (6.1)	0 (0.0)	0 (0.0)	0 (0.0)
Gastroesophageal reflux	2 (6.1)	0 (0.0)	0 (0.0)	0 (0.0)
Hyperhidrosis	2 (6.1)	0 (0.0)	1 (2.9)	0 (0.0)
Hypophosphatemia	2 (6.1)	0 (0.0)	3 (8.6)	1 (2.9)
Musculoskeletal chest pain	2 (6.1)	0 (0.0)	2 (5.7)	0 (0.0)
Myalgia	2 (6.1)	0 (0.0)	2 (5.7)	0 (0.0)
Edema peripheral	2 (6.1)	1 (3.0)	1 (2.9)	0 (0.0)
Osteoarthritis	2 (6.1)	0 (0.0)	2 (5.7)	0 (0.0)
Rash	2 (6.1)	0 (0.0)	4 (11.4)	0 (0.0)
Vomiting	2 (6.1)	0 (0.0)	4 (11.4)	0 (0.0)
Abdominal pain	1 (3.0)	0 (0.0)	3 (8.6)	1 (2.9)
AST increased	1 (3.0)	0 (0.0)	2 (5.7)	1 (2.9)
Blood creatinine increased	1 (3.0)	0 (0.0)	2 (5.7)	0 (0.0)
Insomnia	1 (3.0)	0 (0.0)	2 (5.7)	0 (0.0)
Dysgeusia	0 (0.0)	0 (0.0)	2 (5.7)	0 (0.0)

NOTE: Adverse events with an incidence of ≥5% of any grade in any treatment category.

Treatment-Related Adverse Events

Immune-related adverse events were observed in patients receiving combination therapy and resolved upon discontinuation of treatment (Table 2). Grade 3 or 4 adverse events were infrequent with ciforadenant monotherapy. There were no treatment- or disease-related deaths while on therapy. At the time of data cutoff, 3% of monotherapy-treated and 17% of combination-treated patients remained on therapy. Sixty-five percent of patients discontinued therapy due to disease progression.

Modulation of A2AR Signaling

Pharmacokinetic and pharmacodynamic studies were conducted in a phase I portion of the study which enrolled patients with multiple different histologies. Signaling through A2AR induces phosphorylation of CREB downstream of protein kinase A activation (27). *In vivo* blocking of the adenosine pathway by ciforadenant was examined by determining whether A2AR on patients' peripheral blood lymphocytes could be stimulated *ex vivo* with the adenosine receptor agonist 5′-N-Ethylcarboxamidoadenosine (NECA), as determined by measurement of phosphorylation of CREB by flow cytometry. There was an exposure–response relationship between plasma drug concentrations and inhibition of CREB phosphorylation (pCREB), with nearly complete inhibition at drug levels exceeding 2,000 ng/mL (Fig. 1A). Pharmacokinetic measurements revealed that plasma C_{min} and C_{max} concentrations exceeding 2,000 ng/mL were consistently achieved at the 100 mg twice-daily dose of ciforadenant, and this dose was selected for efficacy evaluation during the expansion stage of this study. There were no significant differences in pharmacokinetics between ciforadenant monotherapy and combination treatment (Supplementary Table S1).

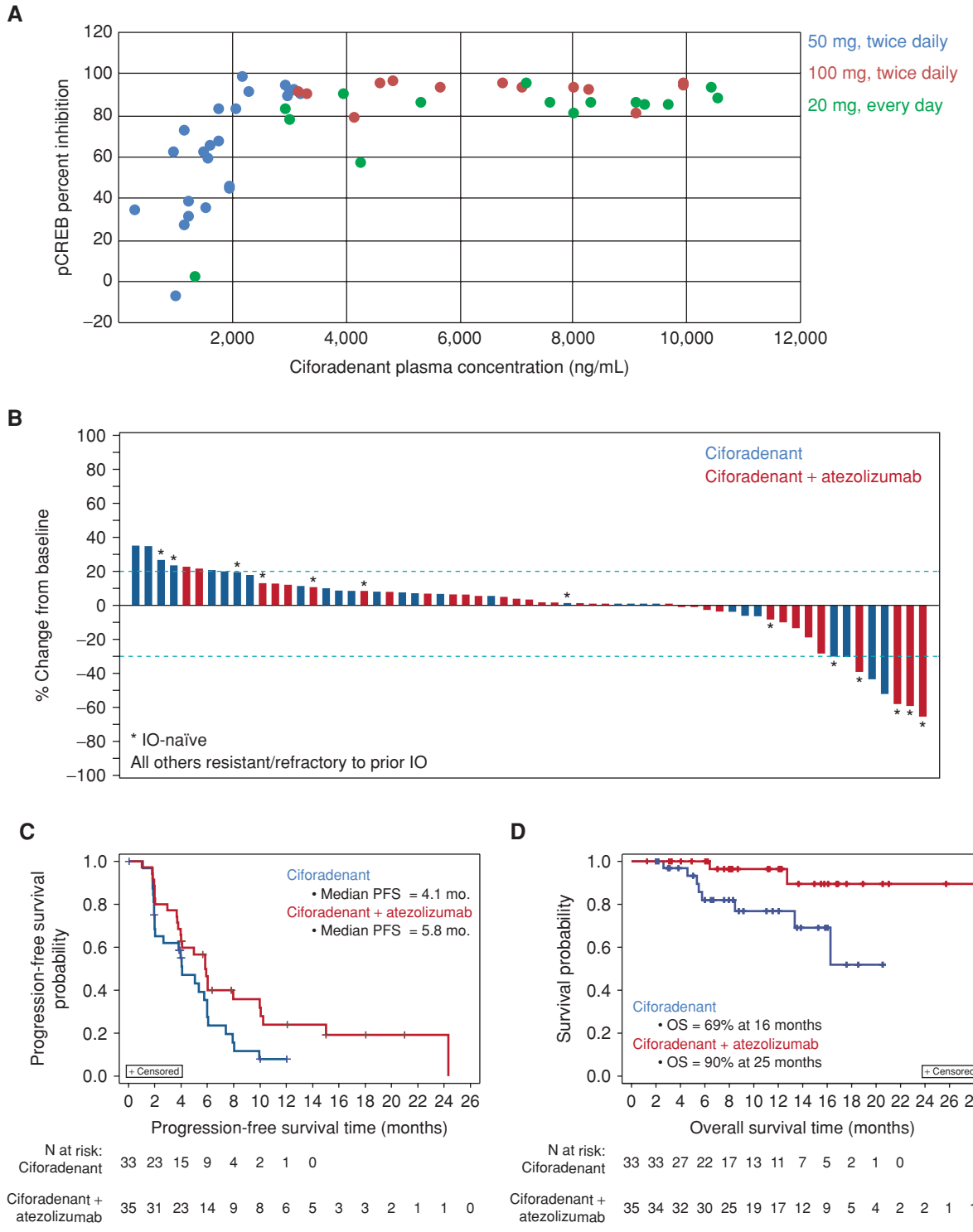

Figure 1. Pharmacokinetics, pharmacodynamics, and tumor response to ciforadenant alone and in combination with atezolizumab. **A,** Blood was collected from subjects with different dosing regimens during an 8-hour time course on treatment day 14 and activated with exogenous 1 μmol/L NECA. Concurrent pharmacokinetic assessments were also performed. The graph shows the relationship between plasma concentration of ciforadenant and inhibition of NECA-induced pCREB, with data from individuals dosed with 50 mg twice daily (blue), 100 mg twice daily (red), or 200 mg every day (green). **B,** Waterfall plot showing best overall response in sum of longest diameter measurements of target lesions. Patients naïve to immunotherapy (IO) at time of enrollment are designated with an asterisk. All others were resistant or refractory to prior immunotherapy treatment. **C** and **D,** Progression-free survival (**C**) and overall survival (**D**) in patients treated with ciforadenant or the ciforadenant plus atezolizumab combination.

Table 3. Six-month disease control rate

	Ciforadenant ($n = 29$)	Ciforadenant + atezolizumab ($n = 33$)
Prior anti–PD-1/PD-L1	25% (5/20)	35% (8/23)
Naïve	0% (0/9)	50% (5/10)
Total	17% (5/29)	39% (13/33)

NOTE: Six-month disease control rates in anti–PD-1/PD-L1-naïve (IO-naïve) and anti–PD-1/PD-L1 resistant/refractory patients treated with ciforadenant or ciforadenant in combination with atezolizumab.

Efficacy

RECIST-defined partial responses were seen in 1 of 33 (3%) patients with RCC treated with ciforadenant monotherapy (Supplementary Fig. S3A) and 4 of 35 (11%) patients with RCC receiving the combination (Supplementary Fig. S3B). An additional 24% (15 of 63 evaluable) of patients experienced tumor regression that did not meet the RECIST criteria for a partial response (Fig. 1B).

Seventeen percent of patients receiving ciforadenant monotherapy and 39% of patients in the combination group had confirmed disease control for at least 6 months (Table 3). The median progression-free survival was 4.1 months and 5.8 months for ciforadenant monotherapy and combination treatment, respectively (Fig. 1C). The estimated overall survival (OS) exceeded 90% at 25 months for the combination group and was more than 69% at 16 months for the ciforadenant monotherapy group (Fig. 1D).

Significant tumor regression was observed in heavily pretreated patients receiving either ciforadenant monotherapy or combination treatment, including patients who failed prior treatment with anti–PD-1/PD-L1 therapy. The median time to best tumor response was 3.4 and 5.5 months for monotherapy and combination, respectively. The kinetics of tumor response were prolonged in some patients as seen in the spider plots (Supplementary Fig. S4). Of note, this included one patient receiving ciforadenant monotherapy who demonstrated initial tumor progression followed by durable tumor regression lasting almost one year (Supplementary Fig. S4) while on continuous therapy. This patient was scored as having progressive disease.

Ciforadenant Efficacy Is Associated with CD8$^+$ T-cell Infiltration

The extent of CD8$^+$ T-cell infiltration present in pretreatment and on-treatment tumor biopsies was evaluated using IHC. Increases in tumor-infiltrating CD8$^+$ T cells were significantly higher in patients with at least 6-month disease control compared with patients with shorter periods of disease control (Fig. 2A, left). Representative images of CD8$^+$ T-cell infiltration into the tumor microenvironment following ciforadenant monotherapy are shown in Fig. 2A (right). We did not observe an association between tumor response and baseline CD8$^+$ T-cell infiltration or CD73 expression, as assayed by both NanoString (Supplementary Figs. S5A, S5B, and S5E) and IHC (Supplementary Fig. S5C–S5E).

Ciforadenant Efficacy Is Associated with Diversification of TCR Repertoire

We have previously shown that CTLA4 blockade can modulate the T-cell receptor (TCR) repertoire (28). The effect of adenosine blockade on the TCR repertoire was investigated by sequencing the TCR Vβ genes in patients receiving ciforadenant alone and in combination with atezolizumab. The Morisita Index, which is a measure of change in TCR repertoire in the peripheral blood on drug treatment, was greater (median = 0.15, SD = 0.23) in subjects with a more diverse baseline TCR repertoire than in subjects with a higher clonality (median = 0.03, SD = 0.01; Fig. 2B). These results would suggest that ciforadenant exerts immunomodulatory effects on the adaptive compartment in patients with broader TCR repertoires that may include preexisting tumor-reactive T cells. Eight of the 13 patients with diverse baseline TCR repertoires, but none of patients with more narrow repertoires, exhibited a Morisita Index above 0.1 compared with post-treatment samples (Fig. 2B), a threshold previously shown to be associated with anti-CTLA4–mediated changes in the TCR repertoire (28). Similar findings were observed in both the ciforadenant monotherapy and the ciforadenant plus atezolizumab combination group.

Responses to Ciforadenant Are Associated with Expression of an Adenosine-Related Gene Signature

It is not practical to routinely measure the concentration of extracellular adenosine in tumors due to its short half-life (plasma $t_{1/2} \leq 10$ seconds; ref. 29). Therefore, we investigated the effects of adenosine on gene expression prolife (GEP) in peripheral blood mononuclear cells (PBMC) to identify a potential molecular surrogate for adenosine exposure in the tumor microenvironment. Adenosine-responsive genes were identified by *in vitro* stimulation of normal human PBMCs with NECA (Supplementary Fig. S6A). A dose-dependent increase in the expression of genes encoding CXCR2 ligands (CXCL1, 2, 3, 5, 8) and mediators of neutrophil/myeloid-derived suppressor cell (MDSC) biology, such as IL23, were observed (Supplementary Table S2; see Supplementary Fig. S6B for graphical representation of analysis). Increased expression of genes encoding monocyte/macrophage inflammatory mediators such as IL1β, IL6, and PTGS2 were also observed, as were increases in CD14, SLC11A1, and THBS1 (Supplementary Table S2). In contrast, *CXCL10* expression was decreased by NECA in a dose-dependent manner (Supplementary Fig. S6B). These gene-expression changes were also reflected in the protein levels of CXCL1, CXCL5 (both increased), and CXCL10 (decreased) in culture supernatants (Fig. 3A and B). Addition of the A2AR antagonist ciforadenant (1 μmol/L) to PBMC cultures fully neutralized the induction of CXCL5 by 0.1 μmol/L and 1 μmol/L NECA, but not at 10 μmol/L NECA (Fig. 3C). This result is expected, as NECA is a much more potent agonist of A2AR (35-fold) and A2BR (72-fold) than adenosine (30). Dose-dependent increases in CCL2, CXCL1, CXCL5, and CXCL8 protein expression were also observed by intracellular flow

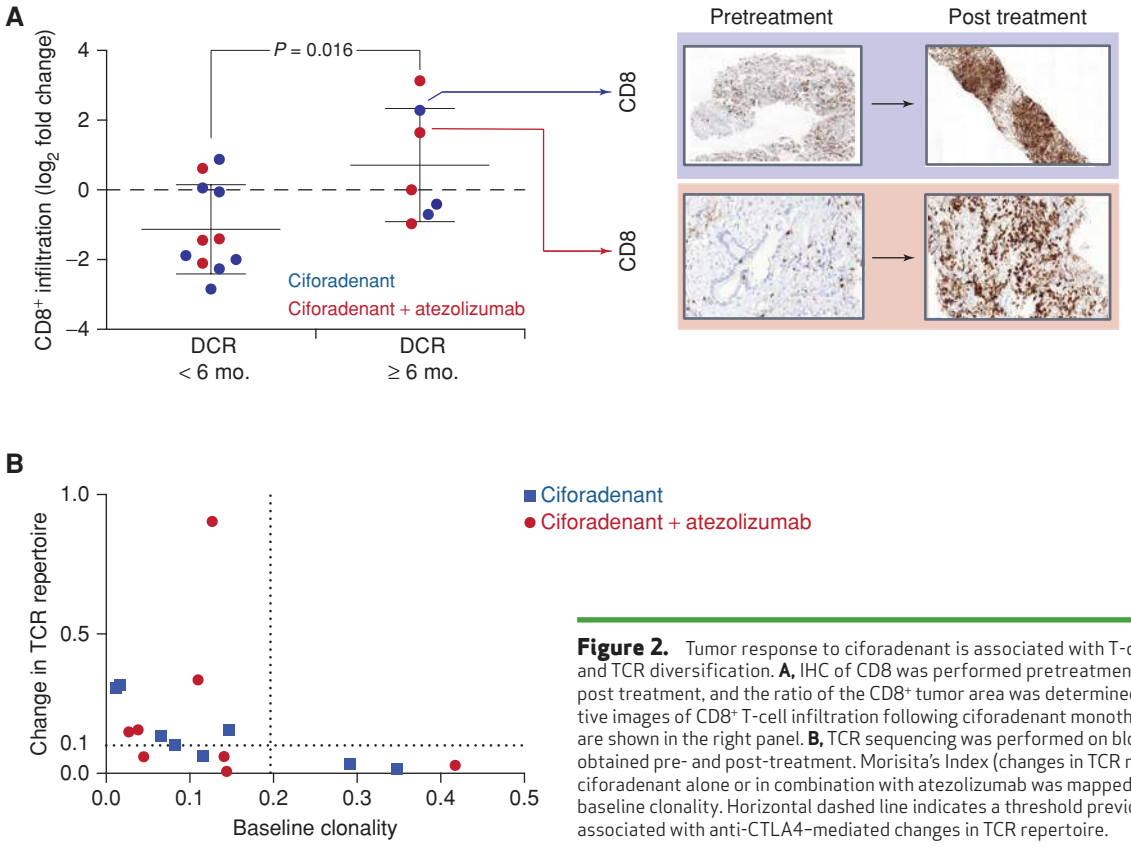

Figure 2. Tumor response to ciforadenant is associated with T-cell infiltration and TCR diversification. **A,** IHC of CD8 was performed pretreatment and 1–4 months post treatment, and the ratio of the CD8+ tumor area was determined. Representative images of CD8+ T-cell infiltration following ciforadenant monotherapy treatment are shown in the right panel. **B,** TCR sequencing was performed on blood samples obtained pre- and post-treatment. Morisita's Index (changes in TCR repertoire) after ciforadenant alone or in combination with atezolizumab was mapped as a function of baseline clonality. Horizontal dashed line indicates a threshold previously shown to be associated with anti-CTLA4–mediated changes in TCR repertoire.

cytometry (Fig. 3D–G). Interestingly, these protein changes occurred specifically in CD14+ monocytes and not CD8+ T cells or CD19+ B cells (Fig. 3D–G), indicating that the source of many adenosine signature chemokines and cytokines is likely to be of monocytic lineage. Our findings suggest that adenosine signaling not only directly dampens T-cell immunity, but also shifts the balance away from T effector responses and toward myeloid suppressor recruitment and functions (25).

We next evaluated the expression of adenosine-induced genes in tumor biopsies collected from 30 patients prior to treatment initiation with ciforadenant alone or in combination with atezolizumab. Patient tumors that demonstrated high levels of adenosine gene signature expression (AdenoSig^{hi}, see Methods: Adenosine Gene Signature in RCC Tumors) were almost exclusively low for an angiogenesis GEP (VEGFA, PECAM1, CD34; Fig. 4A). Gene expression of markers for baseline T-cell activation associated with neither tumor response nor expression of the AdenoSig (Fig. 4A). High levels (top two tertiles) of AdenoSig expression in baseline tumor biopsies was significantly associated with tumor regression (Fig. 4B; $P < 0.008$). These AdenoSig^{hi} patients also demonstrated more durable progression-free survival (PFS); the tail of the PFS curve (40+ weeks) was comprised of 5 of 16 subjects with high AdenoSig expression compared with 0 of 8 with little or no expression (Fig. 2C). These results suggest ciforadenant antitumor activity in RCC is associated with high levels of expression of the AdenoSig in pretreatment biopsies and that the AdenoSig may be useful as a predictive biomarker to select patients more likely to respond to agents that antagonize adenosine production or signaling.

DISCUSSION

This is the first clinical report confirming the activity of adenosine pathway antagonism for cancer immunotherapy. Patients in this trial were often resistant or refractory to anti–PD-1/PD-L1 antibodies, and had predominantly PD-L1–negative tumors, suggesting that these patients harbored tumors that were not immune-suppressed through the PD-1/PD-L1 axis. The A2AR antagonist ciforadenant demonstrated monotherapy activity in immunotherapy-naïve patients as well as patients who were resistant or refractory to prior anti–PD-1/PD-L1 treatment. Although this trial was not designed to compare monotherapy to the combination, treatment with ciforadenant plus atezolizumab appeared to improve efficacy and resulted in a partial response rate of 11%, a 6-month disease control rate (DCR) of 39%, PFS of 5.8 months, and 90% OS at 25 months. Ciforadenant treatment was well tolerated, both alone and in combination with atezolizumab. The observations of antitumor activity of ciforadenant in RCC are consistent with several biological observations, including a significant association between the adenosine-related gene-expression signature and tumor response. We also observed an association with T-cell infiltration induced by treatment and prolonged disease control. TCR diversity was also more frequently increased in patients following treatment.

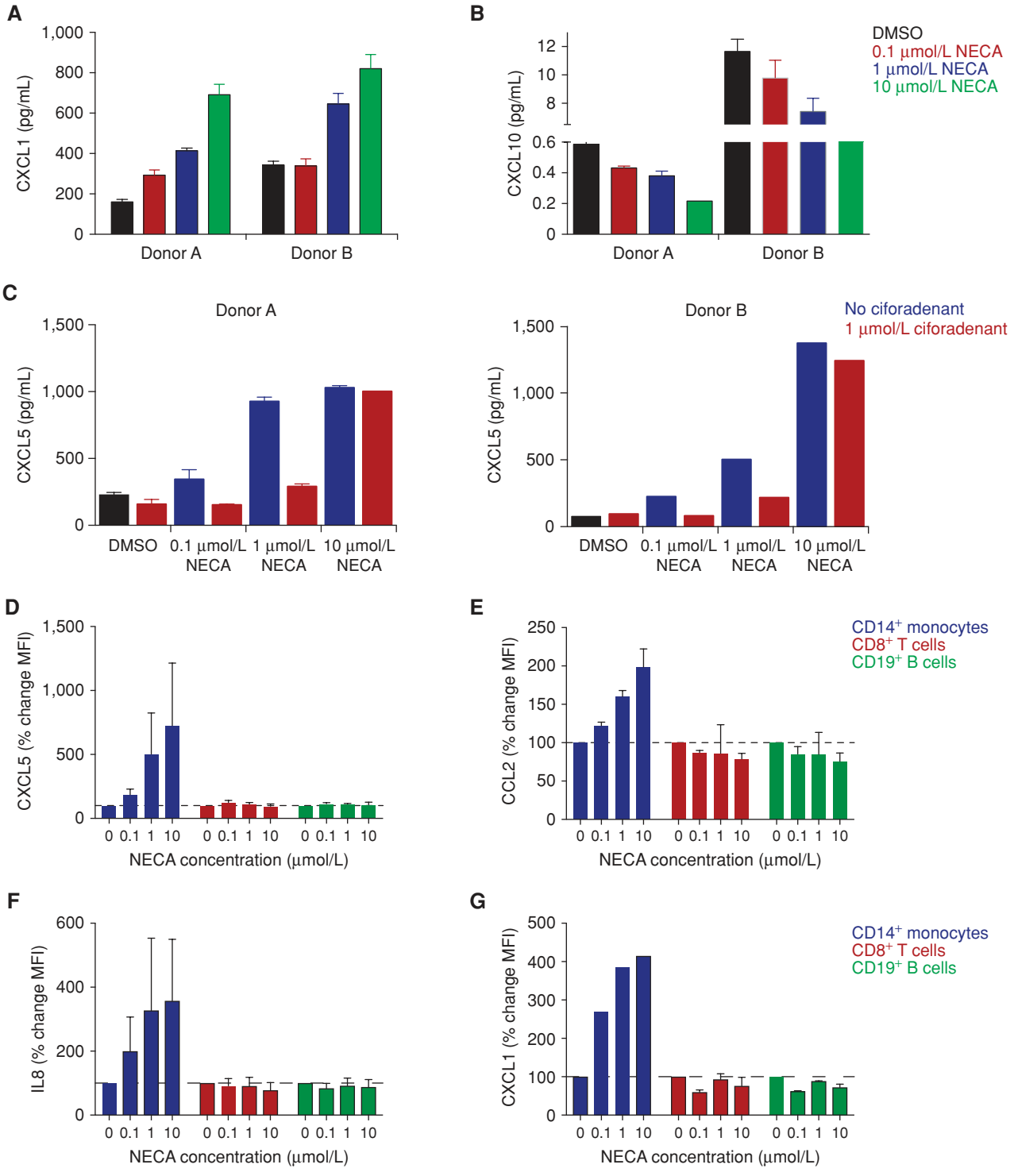

Figure 3. *In vitro* characterization of gene-expression signature related to adenosine exposure. **A** and **B,** Adenosine signature–related chemokine concentrations exhibited a dose-dependent increase (CXCL1; **A**) or decrease (CXCL10; **B**). **C,** Addition of ciforadenant (1 µmol/L) neutralizes the induction of CXCL5 by NECA as determined by ELISA. **D–G,** Purified human PBMCs from healthy donors were cocultured with the indicated concentrations of NECA and were stimulated with anti-human CD3 and CD28 antibodies. Cells were kept in culture for 2 days. Golgi block was added 4 hours prior to collecting cells for intracellular flow cytometry analysis. $CD14^+$ monocytic cells exhibited elevated expression of adenosine signature [as determined by mean fluorescence intensity (MFI)] related cytokines and chemokines including CXCL5 (**D**), CCL2 (**E**), IL8 (**F**), and CXCL1 (**G**) as NECA concentration increased. Lymphocytes including $CD8^+$ T cells and $CD19^+$ B cells had minimal changes. Error bars, SEM.

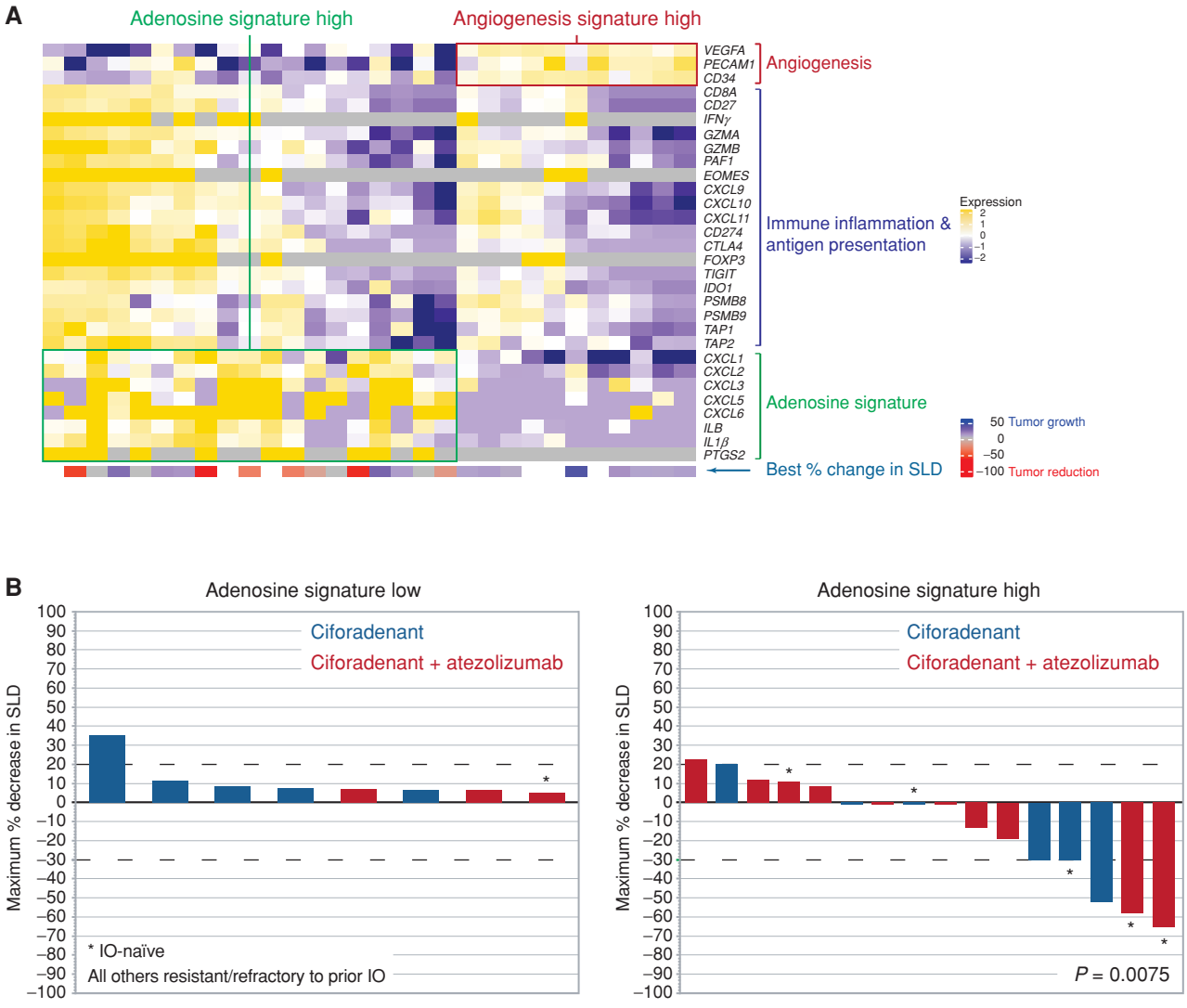

Figure 4. Tumor response to ciforadenant is associated with expression of an adenosine gene-expression signature. **A,** Genes of interest (rows) were assessed from tumors collected pretreatment from 30 patients (columns). Gene expression was *Z*-score transformed with high (yellow) and low (purple) expression normalized for each gene. The median expression of *IFNG*, *EOMES*, *FOXP3*, and *PTGS2* was equivalent to the noise floor so for these genes expression at the noise floor is colored gray and above the noise floor is yellow. Genes are grouped by biological functions of angiogenesis (orange), immune and antigen presentation (blue), and adenosine signature (green). **B,** The waterfall plot shows the best change in the sum of the longest dimensions for patients with low (left) or high (right) expression of the adenosine signature. IO, immunotherapy; SLD, sum of longest dimensions.

Of interest in this study is the finding of encouraging disease control and survival benefit without high objective response rates. As recently reported by others in a large meta analysis of 87 clinical trials of solid tumors treated with immune checkpoint inhibitors, there is a lack of correlation between response rate and survival (31). The reasons for this are uncertain, but it could be due to the triggering of a persistent immune response that maintains durable tumor growth control despite the absence of an immediate elimination of tumor cells. Response rates may also be underestimated on account of the inherent problems of differentiating between tumor cell volume and residual inflammation and fibrosis following tumor elimination by CT scan.

In this study, we characterized an adenosine-related gene-expression signature in tumor biopsies as a surrogate biomarker to identify patients with adenosine-rich tumors (Fig. 4A and B). *In vitro* stimulation of human PBMCs with A2AR agonists enabled us to identify a specific gene signature which in biopsies from patients with RCC was associated with tumor responses to ciforadenant alone or in combination with atezolizumab. The efficacy data presented here suggest that resistance to anti–PD-1/PD-L1 may be reversed by ciforadenant in the AdenoSig^{hi} patients. Indeed, 72% of the patients with RCC enrolled in our study had received prior anti–PD-1/PD-L1 therapy. In preclinical studies, treatment with anti–PD-1 led to increases in A2AR and CD73 expression and was associated with enhanced tumor responses to A2AR blockade (24). In addition, CD38-mediated production of adenosine has been shown to suppress antitumor immunity following anti–PD-1 treatment (32). It is currently

unclear whether adenosine-mediated resistance to checkpoint blockade exists at the time of tumor diagnosis or evolves as a resistance mechanism during the course of anti–PD-1/PD-L1 treatment. Interestingly, our AdenoSig substantially overlaps with an independently derived "myeloid inflammation" signature that was negatively associated with PFS following first-line treatment with atezolizumab in RCC (21). We also found that high expression of the AdenoSig identified patients with low expression of an angiogenesis gene signature; low angiogenesis gene expression is associated with inferior PFS following treatment with sunitinib (21, 33). We therefore hypothesize that the AdenoSig^{hi} patients will be poor responders to antiangiogenesis agents due to the low expression of angiogenesis genes and expect ciforadenant plus anti–PD-1/PD-L1 treatment to compare favorably to such agents.

The studies reported here with ciforadenant confirm the immune-enhancing and therapeutic potential of adenosine pathway blockade. Several other antagonists of A2AR and A2BR are currently under active clinical evaluation, both as monotherapies and in combination with PD-1 blockade, chemotherapy, or targeted agents. Early preliminary data has revealed signs of clinical activity in RCC, non–small cell lung cancer (NSCLC), prostate cancer, endometrial cancer, anal cancer, and head and neck cancer (34–37). In many cases, these treatments have demonstrated activity in both immunotherapy-naïve and resistant/refractory patients. These promising results validate the adenosine axis as a viable immunotherapy target, but more data will be required to determine which molecule or which combinations will be most effective, and what biomarker assays will be most informative.

The patients enrolled in this trial were heavily pretreated, with a median of 3 prior treatments (range 1–5). It is possible that ciforadenant and other adenosine pathway antagonists will be most effective when used in earlier lines of therapy where the immune system is less compromised from prior immunosuppressive regimens. Previous studies in preclinical mouse models have suggested that the efficacy of adenosine pathway antagonists may be predicated on the presence of a sufficient number of antitumor T cells (2). Although it is not yet possible to prospectively screen patients to ensure a specific frequency or distribution of tumor-reactive T cells, an alternative strategy may be to administer ciforadenant in combination with chimeric antigen receptor T cells or *ex vivo* amplified tumor-infiltrating lymphocytes to exogenously supplement tumor-reactive T cells. We note that ciforadenant treatment potentiated the generation of novel T-cell clones appearing in the peripheral blood; however, more studies will be required to determine whether this effect alone is robust enough to generate an effective supply of antitumor T cells in otherwise deficient patients or if the T cell–autonomous effects of A2AR blockade are more prominent in preclinical models.

The unique mechanism of action and favorable safety profile suggest that ciforadenant may be valuable, particularly in patients who have failed anti–PD-1/PD-L1 therapy or in combination with PD-1/PD-L1 blockade to prevent the development of resistance. Although our study combined ciforadenant with a PD-L1 antagonist, there is compelling preclinical evidence for combining adenosine pathway antagonists with other immunotherapies, chemotherapy, and tumor vaccines (8, 23, 24, 26, 38–44). Recent success combining anti–PD-1 with TKIs and other angiogenesis inhibitors suggests there is rationale to explore triplet combination involving ciforadenant to further enhance responses (21, 45, 46). Future studies are also expected to evaluate the utility of the AdenoSig as a predictive biomarker to select patients most likely to benefit from treatments based on adenosine blockade.

METHODS

Patients

In the phase Ia portion of the study, patients at least 18 years of age were eligible for enrollment if they had NSCLC, clear-cell RCC, melanoma, triple negative breast cancer, bladder cancer, prostate cancer, head and neck cancer, or colorectal cancer (microsatellite instability–high), and had failed approved therapies for their cancers (NCT02655822). Eastern Cooperative Oncology Group (ECOG) performance status of 0 or 1 and adequate hematologic, hepatic, and renal functions were required. Prior treatment with an anti–PD-1/PD-L1 or anti-CTLA4 antibody was allowed. PD-L1 expression in the tumor was not used to select patients. This open-label, multicenter, phase I/Ib trial enrolled patients in 30 centers in the United States, Canada, and Australia (see protocol design in Supplementary Fig. S2). Ciforadenant was evaluated at 50 mg and 100 mg twice a day for 14 days and 28 days; 200 mg once a day for 14 days, of a 28-day cycle. In patients receiving the combination, atezolizumab was given 840 mg intravenously every 14 days. The analysis of pharmacokinetics and pharmacodynamics was performed in patients from the phase Ia portion of the study. The selected dose of ciforadenant for the phase Ib portion was 100 mg twice daily for 28 days as monotherapy and in combination with atezolizumab. Both RCC monotherapy and combination cohorts were expanded per protocol based on the demonstration of early signs of efficacy, defined as observing one or more responses in the first 11 patients (Supplementary Fig. S3). All patients with RCC who were enrolled in the phase Ib portion of the trial are included in the safety, efficacy, and biomarker analyses reported here (see Supplementary Fig. S3 for overall trial design).

Patients were followed for safety during treatment and follow-up and every two to three months for investigator-assessed tumor response using RECIST version 1.1. Responses and stable disease required confirmation by subsequent CT scan. All patients continued treatment until confirmed disease progression or unacceptable toxicity. At investigators' discretion, patients with disease progression could continue on therapy if they were thought to be deriving clinical benefit. Objective response (DCR, complete or partial response, or stable disease for ≥ 3 months) and duration of response were evaluated. PFS and OS were calculated using Kaplan–Meier analysis (47).

The study was designed by the sponsor (Corvus Pharmaceuticals) and academic advisors. This trial was performed in accordance with the ethics and principles of the Declaration of Helsinki and the International Council for Harmonisation Good Clinical Practice Guidelines. All patients provided written informed consent. The protocol and informed consent forms were approved by an institutional review board or independent ethics committee at each study site. The data were collected and analyzed by the sponsor and reviewed by a data and safety monitoring committee that consisted of members from the sponsor and independent reviewers. The manuscript was written, reviewed, and approved by the authors. ClinicalTrials.gov number is NCT02655822.

Pharmacokinetic and Pharmacodynamic Measurements

Blood was collected prior to treatment initiation and again on day 14 just prior to administration, and at 1.5 hours, 3 hours,

5 hours, and 8 hours postadministration of ciforadenant. The concentration of ciforadenant was determined by LC/MS-MS following protein precipitation from plasma with methanol/acetonitrile using an internal standard/peak area method. For assessment of A2AR occupancy with ciforadenant, pCREB measurements were conducted by flow cytometric analysis in whole blood that was stimulated with 1 μmol/L of the stable adenosine analogue NECA (Sigma-Aldrich) for 15 minutes. Cells were then fixed (Lyse/Fix buffer from Becton Dickinson) and stored in methanol at −80°C for flow cytometry with antibodies including anti-CD19 (Becton Dickinson) and anti-pCREB (Cell Signaling Technology).

Assessment of PD-L1, CD8, and CD73 Expression

Core-needle tumor biopsies were collected prior to therapy and while on treatment (range 1–4 months on treatment, median 1.5 months), and fixed in formalin, embedded in paraffin, and processed into 5-μm sections. IHC for PD-L1 protein expression was performed using the Ventana PD-L1 (SP142) assay (Ventana), and scored using a cutoff of 5% tumor cell or immune cell staining and positivity according to the diagnostic label for the assay. CD8 clone C8/144B was used to evaluate CD8-positive cell staining (HistoGeneX). To calculate the change in $CD8^+$ T-cell infiltration, a noise floor of 0.5% was applied to the percentage of the tumor area positive for CD8 staining, and then $\log_2$ (the area of on-treatment $CD8^+$/pretreatment $CD8^+$) was calculated for each patient with paired biopsies. An unpooled two-tailed *t* test was performed comparing the patients with DCR < 6 months and DCR ≥ 6 months to calculate the *P* value. CD73 clone D7F9A was used to evaluate CD73-positive cell staining (HistoGeneX).

Analysis of CD73 and A2AR Expression in Tumors

RNA sequencing gene-expression data from The Cancer Genome Atlas was downloaded from the cBioPortal (http://www.cbioportal.org). cBioPortal processed and normalized the data using RSEM to translate the raw data into transcripts per million. For each indication, median tumor expression levels were calculated, as well as 2.5% and 97.5% percentiles for plotting the 95% confidence intervals. Average expression levels for *ADORA2A* and *NT5E* were determined by calculating the mean expression within each indication, and then calculating the mean of all indications.

TCR Repertoire Analysis

Sequencing of the CDR3 regions of human TCRβ chains was performed using the immunoSEQ Assay (Adaptive Biotechnologies). Extracted genomic DNA was amplified in a bias-controlled multiplex PCR, followed by high-throughput sequencing and the abundance of each unique TCRβ CDR3 region was quantified (48–50).

Adenosine Gene Signature

Human PBMCs were isolated from buffy coat samples by density centrifugation with Histopaque 1077 (400 × *g*, 30 minutes). Cells were washed and resuspended at a density of 2×10^6 cells/mL in RPMI + 10% human serum (Sigma-Aldrich, catalog no. H4522). PBMCs (10 mL) were stimulated with DMSO or NECA (Tocris, catalog no. 1691) at 0.1, 1, or 10 μmol/L for 1 hour. T cells were then activated with anti-CD3 (clone HIT3a, 1 μg/mL) and anti-CD28 (clone CD28.2, 1 μg/mL) antibodies and incubated for 48 hours at 37°C. Purified RNA was collected using a Qiagen RNAEasy Kit according to the manufacturer's protocol. NanoString analysis was performed according to the manufacturer's protocol on a NanoString Sprint instrument using the NanoString PanCancer Immune Profiling Panel with PLUS codeset. Normalized counts were obtained using NanoString nSolver Software. Log_2-transformed expression data were fit to a linear model comprised of donor and treatment effects. Genes that showed a statistically significant treatment effect (i.e., gene-expression level increased or decreased as NECA level increased) were identified in three initial donors. P_{adj} values were used to correct for multiple hypothesis testing using the Benjamini–Hochberg procedure. Cuture supernatants from three donors were assessed with the human CXCL5 ELISA Kit (R&D Systems, DX000).

Intracellular Flow Cytometry

Purified human PBMCs from three healthy donors were cocultured with various concentrations of NECA and were stimulated with anti-human CD3 and CD28 antibody (at 1 μg/mL). Cells were kept in culture for 48 hours. Golgi block was added 4 hours prior to intracellular flow cytometry analysis. Antibodies used in analysis included anti-human CD8a (clone RPA-T8, BioLegend catalog no. 301048), anti-human CD3 (clone OKT3, BioLegend, catalog no. 317322), anti-human CD4 (clone OKT4, BioLegend, catalog no. 317436), anti-human CD56 (clone 5.1H11, BioLegend, catalog no. 362546), anti-human CD205 (clone HD30, BioLegend, catalog no. 342210), anti-human CD14 (clone 63D3, BioLegend, catalog no. 367118), anti-human CD19 (clone SJ25C1, BioLegend, catalog no. 363034), anti-human CXCL5 (clone J111B7, BioLegend, catalog no. 524104), anti-human MCP1 (clone 2H5, BioLegend, catalog no. 505904), anti-human IL8 (clone E8N1, BioLegend, catalog no. 511408), and anti-human CXCL1 (clone 20326, R&D Systems, catalog no. IC275P). Data was acquired on a CytoFLEX flow cytometer (Beckman Coulter) and analyzed in FlowJo software v10.

Adenosine Gene Signature in RCC Tumors

Tumor biopsies were obtained from patients with RCC prior to treatment. RNA was extracted from tumor tissue macrodissected from 5-μm sections cut from formalin-fixed paraffin-embedded specimens. Seventy to 100 ng of purified RNA was analyzed on the NanoString Sprint instrument using the PanCancer Immune Profiling Panel (NanoString) at HistoGeneX. NanoString data was normalized to housekeeping genes, and bridging of normalized data between NanoString codeset lots was performed. A noise floor of 30 counts was applied to normalized and bridged NanoString data.

The expression of eight NECA-induced immune-related genes (encoding IL1β, PTGS2, and CXCL1, 2, 3, 5, 6, 8) were selected to comprise the AdenoSig because they were expressed at detectable levels in the patient tumor samples from this study and were found to be significantly induced in normal PBMCs upon exposure to NECA. AdenoSig gene-expression profile scores were calculated as the mean of the $\log_2$ value of the counts for each gene component. The distribution of the adenosine signature for all evaluated patients with RCC was determined, and a cut-off point at the first tertile was selected as optimal to differentiate patients with low expression from high expression. An unpooled two-tailed *t* test was performed to calculate the *P* value for the comparison between the AdenoSig^{lo} and AdenoSig^{hi} patient groups for the best change in the sum of the longest dimensions of the target lesions. Normalized gene-expression data was *Z*-scale transformed for heat-map visualization.

Disclosure of Potential Conflicts of Interest

L. Fong reports receiving commercial research grants from AbbVie, Bavarian Nordic, Bristol-Myers Squibb, Dendreon, Janssen, Merck, and Roche/Genentech and has ownership interest (including patents) in Atreca, Nutcracker, and Teneobio. A. Hotson is a scientist at Corvus Pharmaceuticals and has ownership interest (including patents) in the same. J.D. Powderly is a founder and president at Carolina BioOncology Institute, PLLC and BioCytics Inc., reports receiving commercial research grants from Bristol-Myers Squibb, Genentech, Corvus Pharmaceuticals, AbbVie, Sequenom, Top Alliance BioSciences, EMD Serono, AstraZeneca, InCyte, Arcus, FLX BioSciences, Alkermes, Tempest, and Curis, reports receiving other commercial research support from Precision Medicine and MT Group, has received speakers

bureau honoraria from Bristol-Myers Squibb, Genentech, and Merck, and has ownership interest (including patents) in Iovance, BioCytics Inc., and Carolina BioOncology Institute, PLLC. M. Sznol is a consultant at AstraZeneca, Bristol-Myers Squibb, Roche/Genentech, Merck US, and Omniox, and has ownership interest (including patents) in Adaptive Biotech. R.S. Heist is a consultant at Boehringer Ingelheim, Novartis, Apollomics, and Tarveda. T.K. Choueiri reports receiving a commercial research grant from Corvus Pharmaceuticals, has received other commercial research support from Bristol-Myers Squibb, Merck, Roche, Exelixis, Pfizer, and Novartis, and has ownership interest (including patents) in Tempest and PionyR. S. George is a consultant at Pfizer, Bristol-Myers Squibb, Bayer, Corvus Pharmaceuticals, EMD Serono, Sanofi, Exelixis, and Genentech. M.D. Hellmann is a consultant at Merck, AstraZeneca, Genentech/Roche, Bristol-Myers Squibb, Nektar, Syndax, Mirati, Shattuck Labs, Immunai, and Blueprint Medicines, reports receiving a commercial research grant from Bristol-Myers Squibb, and has ownership interest in a patent filed by Memorial Sloan Kettering (PCT/US2015/062208) for the use of tumor mutation burden for prediction of immunotherapy efficacy, which is licensed to Personal Genome Diagnostics, Immunai, and Shattuck Labs. B.I. Rini is a consultant at Corvus Pharmaceuticals, Pfizer, Merck, Roche, BMS, Arravive, 3D Medicines, and Surface Oncology and reports receiving commercial research grants from Corvus, Merck, Pfizer, Roche, Bristol-Myers Squibb, and AstraZeneca. S. Kummar is a member of the data safety monitoring committee at Corvus Pharmaceuticals. L.A. Emens is a member of the board of directors at the Society for Immunotherapy of Cancer, reports receiving commercial research grants from F. Hoffmann La Roche, Genentech, Aduro Biotech, AstraZeneca, Bristol-Myers Squibb, Corvus Pharmaceuticals, EMD Serono, HeritX, Incorporated, Maxcyte, and Merck, has ownership interest (including patents) in Aduro Biotech, and is a consultant/advisory board member for F. Hoffmann La Roche, Genentech, Roche, Syndax, Lilly, Peregrine, Pfizer, eTHeRNA, AbbVie, Bayer, Bristol-Myers Squibb, Gritstone, Medimmune, Molecuvax, Macrogenics, and Replimmune. D. Mahadevan is IRC Chair at Pfizer and a data safety consultant at TG Therapeutics and has received speakers bureau honoraria from Guardant Health. J.J. Luke is a consultant at TTC Oncology, 7 Hills, Array, Astellas, AstraZeneca, Bayer, Bristol-Myers Squibb, Compugen, EMD Serono, IDEAYA, Immunocore, Incyte, Actym, Janssen, Merck, Mersana, Novartis, RefleXion, Vividion, Akrevia, Alphamab Oncology, Mavu, Pyxis, Springbank, Tempest, and AbbVie, reports receiving commercial research grants from Array, CheckMate, Evelo, and Palleon, and has ownership interest (including patents) in Actym, Alphamab Oncology, Mavu, Pyxis, and Tempest. G. Laport has ownership interest (including patents) in Corvus Pharmaceuticals. J.D. Brody reports receiving commercial research grants from Merck, Genentech, Acerta Pharma, Kite Pharma, Celgene, Celldex Therapeutics, Seattle Genetics, and Janssen. L. Hernandez-Aya is a consultant/advisory board member for Bristol-Myers Squibb and has received speakers bureau honoraria from Regeneron. P. Bonomi is a consultant/advisory board member for AstraZeneca, Biodesix, Merck, and Pfizer. J.W. Goldman is a consultant at AstraZeneca and Genentech, reports receiving commercial research grants from BMS, Genentech, and AstraZeneca, and has received speakers bureau honoraria from Merck. D.J. Renouf has received speakers bureau honoraria from Celgene, Roche, Servier, AstraZeneca, and Taiho. R.A. Goodwin is a consultant/advisory board member for Ipsen, Novartis, AAA, Amgen, and Tahio, reports receiving commercial research grants from Ipsen, Novartis, and Apobiologix, and has received speakers bureau honoraria from Amgen. B. Munneke is a director of biostatistics at Corvus Pharmaceuticals and has ownership interest (including patents) in the same. P.Y. Ho is a senior research associate at Corvus Pharmaceuticals and has ownership interest (including patents) in the same. J. Hsieh is a research associate at Corvus Pharmaceuticals and has ownership interest (including patents) in the same. I. McCaffery is a VP, translational sciences at Corvus Pharmaceuticals and has ownership interest (including patents) in the same. L. Kwei is a VP of biometrics and clinical operations at Corvus Pharmaceuticals Inc. S.B. Willingham is a senior scientist II at Corvus Pharmaceuticals and has ownership interest (including patents) in the same. R.A. Miller is CEO at, reports receiving a commercial research grant from, and has ownership interest (including patents) in Corvus Pharmaceuticals. No potential conflicts of interest were disclosed by the other authors.

Authors' Contributions

Conception and design: L. Fong, T.K. Choueiri, S. George, B.I. Rini, G. Laport, J.D. Brody, I. McCaffery, L. Kwei, S.B. Willingham, R.A. Miller

Development of methodology: L. Fong, B.I. Rini, D. Mahadevan, G. Laport, J.D. Brody, I. McCaffery, L. Kwei, S.B. Willingham, R.A. Miller

Acquisition of data (provided animals, acquired and managed patients, provided facilities, etc.): L. Fong, J.D. Powderly, M. Sznol, R.S. Heist, T.K. Choueiri, S. George, B.G.M. Hughes, M.D. Hellmann, D.R. Shepard, B.I. Rini, S. Kummar, A.M. Weise, M.J. Riese, B. Markman, L.A. Emens, D. Mahadevan, J.J. Luke, J.D. Brody, L. Hernandez-Aya, P. Bonomi, J.W. Goldman, L. Berim, D.J. Renouf, R.A. Goodwin, P.Y. Ho, J. Hsieh, I. McCaffery, L. Kwei, S.B. Willingham, R.A. Miller

Analysis and interpretation of data (e.g., statistical analysis, biostatistics, computational analysis): L. Fong, A. Hotson, R.S. Heist, S. George, M.D. Hellmann, B.I. Rini, S. Kummar, A.M. Weise, B. Markman, L.A. Emens, D. Mahadevan, J.J. Luke, G. Laport, J.D. Brody, J.W. Goldman, B. Munneke, P.Y. Ho, I. McCaffery, L. Kwei, S.B. Willingham, R.A. Miller

Writing, review, and/or revision of the manuscript: L. Fong, A. Hotson, J.D. Powderly, M. Sznol, R.S. Heist, T.K. Choueiri, S. George, B.G.M. Hughes, M.D. Hellmann, D.R. Shepard, B.I. Rini, S. Kummar, A.M. Weise, M.J. Riese, B. Markman, L.A. Emens, D. Mahadevan, J.J. Luke, G. Laport, J.D. Brody, L. Hernandez-Aya, J.W. Goldman, D.J. Renouf, R.A. Goodwin, I. McCaffery, L. Kwei, S.B. Willingham, R.A. Miller

Administrative, technical, or material support (i.e., reporting or organizing data, constructing databases): L. Fong, J.D. Brody, P.Y. Ho, I. McCaffery, R.A. Miller

Study supervision: L. Fong, T.K. Choueiri, S. George, B.I. Rini, A.M. Weise, G. Laport, J.D. Brody, I. McCaffery, L. Kwei

Acknowledgments

We thank Jennifer Law, Raj Phadtare, Chris Clark, Gabriel Luciano, and other members of the Corvus clinical operations team, Cindy Wilson and Janet Koe for regulatory support and project management, Chunyan Gu for assistance with biosample management, Erik Evensen and J. Ireland for bioinformatic support, Ben Jones, Jingrong Xu, Felicia Flicker, and Liang Liu for drug supply and DMPK support, Katherine Woodworth and Brandon Dezewiecki for administrative and facilities support, Leiv Lea and the Corvus finance team for budgetary oversight, and Erik Verner and Zhihong Li for thoughtful discussions. Genentech provided atezolizumab for this trial. Clinical trial and associated biomarker research funded by Corvus Pharmaceuticals. L. Fong is supported by NIHR01CA223484 and U01CA233100.

Received August 23, 2019; revised October 15, 2019; accepted November 7, 2019; published first November 15, 2019.

REFERENCES

1. Sharma P, Hu-Lieskovan S, Wargo JA, Ribas A. Primary, adaptive, and acquired resistance to cancer immunotherapy. Cell 2017;168:707–23.

2. Ohta A, Gorelik E, Prasad SJ, Ronchese F, Lukashev D, Wong MK, et al. A2A adenosine receptor protects tumors from antitumor T cells. Proc Natl Acad Sci U S A 2006;103:13132–7.
3. Sitkovsky MV, Hatfield S, Abbott R, Belikoff B, Lukashev D, Ohta A, et al. Hostile, hypoxia-A2-adenosinergic tumor biology as the next barrier to overcome for tumor immunologists. Cancer Immunol Res 2014;2:598–605.
4. Ohta A, Sitkovsky M. Role of G-protein-coupled adenosine receptors in downregulation of inflammation and protection from tissue damage. Nature 2001;414:916–20.
5. Lokshin A, Raskovalova T, Huang X, Zacharia LC, Jackson EK, Gorelik E. Adenosine-mediated inhibition of the cytotoxic activity and cytokine production by activated natural killer cells. Cancer Res 2006;66:7758–65.
6. Raskovalova T, Lokshin A, Huang X, Jackson EK, Gorelik E. Adenosine-mediated inhibition of cytotoxic activity and cytokine production by IL-2/NKp46-activated NK cells: involvement of protein kinase A isozyme I (PKA I). Immunol Res 2006;36:91–9.
7. Young A, Ngiow SF, Gao Y, Patch AM, Barkauskas DS, Messaoudene M, et al. A2AR adenosine signaling suppresses natural killer cell maturation in the tumor microenvironment. Cancer Res 2018;78:1003–16.
8. Beavis PA, Divisekera U, Paget C, Chow MT, John LB, Devaud C, et al. Blockade of A2A receptors potently suppresses the metastasis of CD73+ tumors. Proc Natl Acad Sci U S A 2013;110:14711–6.
9. Cekic C, Linden J. Adenosine A2A receptors intrinsically regulate CD8+ T cells in the tumor microenvironment. Cancer Res 2014;74:7239–49.
10. Maj T, Wang W, Crespo J, Zhang H, Wang W, Wei S, et al. Oxidative stress controls regulatory T cell apoptosis and suppressor activity and PD-L1-blockade resistance in tumor. Nat Immunol 2017;18:1332.
11. Zarek PE, Huang CT, Lutz ER, Kowalski J, Horton MR, Linden J, et al. A2A receptor signaling promotes peripheral tolerance by inducing T-cell anergy and the generation of adaptive regulatory T cells. Blood 2008;111:251–9.
12. Mandapathil M, Hilldorfer B, Szczepanski MJ, Czystowska M, Szajnik M, Ren J, et al. Generation and accumulation of immunosuppressive adenosine by human CD4+CD25highFOXP3+ regulatory T cells. J Biol Chem 2010;285:7176–86.
13. Sitkovsky MV. T regulatory cells: hypoxia-adenosinergic suppression and re-direction of the immune response. Trends Immunol 2009;30:102–8.
14. Antonioli L, Blandizzi C, Pacher P, Haskó G. Immunity, inflammation and cancer: a leading role for adenosine. Nat Rev Cancer 2013;13:842–57.
15. Hatfield SM, Kjaergaard J, Lukashev D, Schreiber TH, Belikoff B, Abbott R, et al. Immunological mechanisms of the antitumor effects of supplemental oxygenation. Sci Transl Med 2015;7:277ra30.
16. Synnestvedt K, Furuta GT, Comerford KM, Louis N, Karhausen J, Eltzschig HK, et al. Ecto-5′-nucleotidase (CD73) regulation by hypoxia-inducible factor-1 mediates permeability changes in intestinal epithelia. J Clin Invest 2002;110:993–1002.
17. Blay J, White TD, Hoskin DW. The extracellular fluid of solid carcinomas contains immunosuppressive concentrations of adenosine. Cancer Res 1997;57:2602–5.
18. Tak E, Jung DH, Kim SH, Park GC, Jun DY, Lee J, et al. Protective role of hypoxia-inducible factor-1alpha-dependent CD39 and CD73 in fulminant acute liver failure. Toxicol Appl Pharmacol 2017;314:72–81.
19. Hatfield SM, Kjaergaard J, Lukashev D, Belikoff B, Schreiber TH, Sethumadhavan S, et al. Systemic oxygenation weakens the hypoxia and hypoxia inducible factor 1alpha-dependent and extracellular adenosine-mediated tumor protection. J Mol Med 2014;92:1283–92.
20. Motzer RJ, Tannir NM, McDermott DF, Arén Frontera O, Melichar B, Choueiri TK, et al. Nivolumab plus ipilimumab versus sunitinib in advanced renal-cell carcinoma. N Engl J Med 2018;378:1277–90.
21. McDermott DF, Huseni MA, Atkins MB, Motzer RJ, Rini BI, Escudier B, et al. Clinical activity and molecular correlates of response to atezolizumab alone or in combination with bevacizumab versus sunitinib in renal cell carcinoma. Nat Med 2018;24:749–57.
22. Choueiri TK, Larkin J, Oya M, Thistlethwaite F, Martignoni M, Nathan P, et al. Preliminary results for avelumab plus axitinib as first-line therapy in patients with advanced clear-cell renal-cell carcinoma (JAVELIN Renal 100): an open-label, dose-finding and dose-expansion, phase 1b trial. Lancet Oncol 2018;19:451–60.
23. Allard B, Pommey S, Smyth MJ, Stagg J. Targeting CD73 enhances the antitumor activity of anti-PD-1 and anti-CTLA-4 mAbs. Clin Cancer Res 2013;19:5626–35.
24. Beavis PA, Milenkovski N, Henderson MA, John LB, Allard B, Loi S, et al. Adenosine receptor 2A blockade increases the efficacy of anti-PD-1 through enhanced antitumor T-cell responses. Cancer Immunol Res 2015;3:506–17.
25. Willingham SB, Ho PY, Hotson A, Hill C, Piccione EC, Hsieh J, et al. A2AR antagonism with CPI-444 induces antitumor responses and augments efficacy to anti-PD-(L)1 and anti-CTLA-4 in preclinical models. Cancer Immunol Res 2018;6:1136–49.
26. Leone RD, Sun IM, Oh MH, Sun IH, Wen J, Englert J, et al. Inhibition of the adenosine A2a receptor modulates expression of T cell coinhibitory receptors and improves effector function for enhanced checkpoint blockade and ACT in murine cancer models. Cancer Immunol Immunother 2018;67:1271–84.
27. He X, Hu JL, Li J, Zhao L, Zhang Y, Zeng YJ, et al. A feedback loop in PPARgamma-adenosine A2A receptor signaling inhibits inflammation and attenuates lung damages in a mouse model of LPS-induced acute lung injury. Cell Signal 2013;25:1913–23.
28. Cha E, Klinger M, Hou Y, Cummings C, Ribas A, Faham M, et al. Improved survival with T cell clonotype stability after anti-CTLA-4 treatment in cancer patients. Sci Transl Med 2014;6:238ra70.
29. Moser GH, Schrader J, Deussen A. Turnover of adenosine in plasma of human and dog blood. Am J Physiol 1989;256:C799–806.
30. de Lera Ruiz M, Lim YH, Zheng J. Adenosine A2A receptor as a drug discovery target. J Med Chem 2014;57:3623–50.
31. Ritchie G, Gasper H, Man J, Lord S, Marschner I, Friedlander M, et al. Defining the Most appropriate primary end point in phase 2 trials of immune checkpoint inhibitors for advanced solid cancers: a systematic review and meta-analysis. JAMA Oncol 2018;4:522–8.
32. Chen L, Diao L, Yang Y, Yi X, Rodriguez BL, Li Y, et al. CD38-mediated immunosuppression as a mechanism of tumor cell escape from PD-1/PD-L1 blockade. Cancer Discov 2018;8:1156–75.
33. Verbiest A, Verbiest A, Couchy G, Job S, de Reynies A, Meiller C, et al. Pro-angiogenic gene expression is associated with better outcome on sunitinib in metastatic clear-cell renal cell carcinoma AU - Beuselinck, Benoit. Acta Oncol 2018;57:498–508.
34. 33rd annual meeting & pre-conference programs of the Society for Immunotherapy of Cancer (SITC 2018). J Immunother Cancer 2018;6:114.
35. Powderly JD, de Souza PL, Gutierrez R, Horvath L, Seitz L, Ashok D, et al. AB928, a novel dual adenosine receptor antagonist, combined with chemotherapy or AB122 (anti-PD-1) in patients (pts) with advanced tumors: preliminary results from ongoing phase I studies. J Clin Oncol 2019;37:2604.
36. Chiappori A, Williams CC, Creelan BC, Tanvetyanon T, Gray JE, Haura EB, et al. Phase I/II study of the A2AR antagonist NIR178 (PBF-509), an oral immunotherapy, in patients (pts) with advanced NSCLC. J Clin Oncol 2018;36:9089.
37. Bendell J, Bauer T, Patel M, Falchook G, Karlix JL, Lim E, et al. Evidence of immune activation in the first-in-human phase Ia dose escalation study of the adenosine 2a receptor antagonist, AZD4635, in patients with advanced solid tumors [abstract]. In: Proceedings of the American Association for Cancer Research Annual Meeting 2019; 2019 Mar 29–Apr 3; Atlanta, GA. Philadelphia (PA): AACR; 2019. Abstract nr CT026.
38. Beavis PA, Henderson MA, Giuffrida L, Mills JK, Sek K, Cross RS, et al. Targeting the adenosine 2A receptor enhances chimeric antigen receptor T cell efficacy. J Clin Invest 2017;127:929–41.
39. Loi S, Pommey S, Haibe-Kains B, Beavis PA, Darcy PK, Smyth MJ, et al. CD73 promotes anthracycline resistance and poor prognosis in triple negative breast cancer. Proc Natl Acad Sci U S A 2013;110:11091–6.
40. Kjaergaard J, Hatfield S, Jones G, Ohta A, Sitkovsky M. A2A adenosine receptor gene deletion or synthetic A2A antagonist liberate tumor-reactive CD8(+) T cells from tumor-induced immunosuppression. J Immunol 2018;201:782–91.

41. Mittal D, Young A, Stannard K, Yong M, Teng MW, Allard B, et al. Antimetastatic effects of blocking PD-1 and the adenosine A2A receptor. Cancer Res 2014;74:3652–8.
42. Iannone R, Miele L, Maiolino P, Pinto A, Morello S. Adenosine limits the therapeutic effectiveness of anti-CTLA4 mAb in a mouse melanoma model. Am J Cancer Res 2014;4:172–81.
43. Waickman AT, Alme A, Senaldi L, Zarek PE, Horton M, Powell JD. Enhancement of tumor immunotherapy by deletion of the A2A adenosine receptor. Cancer Immunol Immunother 2012;61:917–26.
44. Beavis PA, Milenkovski N, Stagg J, Smyth MJ, Darcy PK. A2A blockade enhances anti-metastatic immune responses. Oncoimmunology 2013;2:e26705.
45. Motzer RJ, Penkov K, Haanen J, Rini B, Albiges L, Campbell MT, et al. Avelumab plus axitinib versus sunitinib for advanced renal-cell carcinoma. N Engl J Med 2019;380:1103–15.
46. Rini BI, Plimack ER, Stus V, Gafanov R, Hawkins R, Nosov D, et al. Pembrolizumab plus axitinib versus sunitinib for advanced renal-cell carcinoma. N Engl J Med 2019;380:1116–27.
47. Kaplan EL, Meier P. Nonparametric estimation from incomplete observations. J Am Stat Assoc 1958;53:457–81.
48. Robins HS, Campregher PV, Srivastava SK, Wacher A, Turtle CJ, Kahsai O, et al. Comprehensive assessment of T-cell receptor beta-chain diversity in alphabeta T cells. Blood 2009;114:4099–107.
49. Robins H, Desmarais C, Matthis J, Livingston R, Andriesen J, Reijonen H, et al. Ultra-sensitive detection of rare T cell clones. J Immunol Methods 2012;375:14–9.
50. Carlson CS, Emerson RO, Sherwood AM, Desmarais C, Chung MW, Parsons JM, et al. Using synthetic templates to design an unbiased multiplex PCR assay. Nat Commun 2013;4:2680.